Icarus 224 (2013) 14–23

Contents lists available at SciVerse ScienceDirect

Icarus

journal homepage: www.elsevier.com/locate/icarus

Earliest recorded ground-based decameter wavelength observations of Saturn's lightning during the giant E-storm detected by Cassini spacecraft in early 2006

A.A. Konovalenko [a,*], N.N. Kalinichenko [a], H.O. Rucker [b], A. Lecacheux [c], G. Fischer [b], P. Zarka [d], V.V. Zakharenko [a], K.Y. Mylostna [a], J.-M. Grießmeier [e], E.P. Abranin [a], I.S. Falkovich [a], K.M. Sidorchuk [a], W.S. Kurth [f], M.L. Kaiser [g], D.A. Gurnett [f]

[a] Institute of Radio Astronomy, 4, Chervonopraporna Str., 61002 Kharkiv, Ukraine
[b] Space Research Institute, Austria, 6, Schmiedlstraße, 8042 Graz, Austria
[c] LESIA, Observatoire de Paris, UMR, CNRS 8109, 92195 Meudon, France
[d] LESIA, Observatoire de Paris, CNRS, UPMC, Université Paris Diderot, 5 Place Jules Janssen, 92190 Meudon, France
[e] LPC2E, 3A, Avenue de la Recherche Scientifique, 45071 Orléans cedex 2, France
[f] Department of Physics and Astronomy, University of Iowa, 203 Van Allen Hall, Iowa City, 52242 IA, USA
[g] NASA Goddard Space Flight Center, 8800 Greenbelt Road, Greenbelt, 20771 MD, USA

ARTICLE INFO

Article history:
Received 21 March 2012
Revised 25 July 2012
Accepted 26 July 2012
Available online 3 September 2012

Keywords:
Saturn
Lightning
Radio observations
Saturn, Atmosphere

ABSTRACT

We report the history of the first recorded ground-based radio detection of Saturn's lightning using the Ukrainian UTR-2 radiotelescope at frequencies from 20 to 25 MHz. The observations were performed between 29 January and 3 February 2006, during which lighting activity (E-storm) on Saturn was detected by the radio experiment onboard Cassini spacecraft. The minimum detectable flux density (1σ-level) at UTR-2 reached 40 Jy ($1\ \text{Jy} = 10^{-26}\ \text{W m}^{-2}\ \text{Hz}^{-1}$) for narrowband observations ($\Delta f = 10$ kHz) and 4 Jy for broadband observations ($\Delta f = 1$ MHz), for an effective telescope area of $\approx 100,000\ \text{m}^2$ and integration time of 20 ms. Selection criteria including comparison of simultaneous ON/OFF-source observations were applied to distinguish detection of lightning-associated radio pulses from interference. This allowed us to identify about 70 events with signal-to-noise ratio more than 5. Measured flux densities (between 50 and 700 Jy) and burst durations (between 60 and 220 ms) are in good agreement with extrapolation of previous Cassini measurements to a ground-based observer. This first detection demonstrates the possibility of Solar System planetary lightning studies using large, present and future ground-based radio instruments. The developed methods of observations and identification criteria are also implemented on the UTR-2 radio telescope for the investigation of the next Saturn's storms. Together with recently published UTR-2 measurements of activity measured after the 2006 storm reported here, the results have significant implications for detectable planetary radio emission in our Solar System and beyond.

1. Introduction

1.1. Radio detection of Saturn's lightning by space missions

Impulsive radio emission from so-called Electrostatic Discharges in Saturn's atmosphere (SED) were first discovered between 1 and 40 MHz by the Voyager 1 Planetary Radio Astronomy experiment in 1980 (Warwick et al., 1981; Evans et al., 1981). Weak bursts similar to SED, which were called UED, were also discovered by Voyager 2 at Uranus (Zarka and Pedersen, 1986). The Radio and Plasma Wave Science (RPWS) instrument onboard Cassini spacecraft allowed to re-observe SED between 2 and 16 MHz during 2004–2006 (Fischer et al., 2006a, 2007).

The properties of SED radio emission relevant for the ground-based study, reported below, are (Zarka and Pedersen, 1983; Zarka et al., 2004, 2006; Fischer et al., 2006b):

- SED are impulsive broadband radio emissions observed in the frequency range from 1 MHz to 40 MHz, and possibly existing at higher and lower frequencies.
- SED spectrum is nearly flat up to 10 or 20 MHz and decreases as $f^{-\gamma}$ with $\gamma = -0.5 \cdots -1$ at higher frequencies.
- The average emitted spectral power of SED is between 50 and 100 W/Hz in the above mentioned frequency range (1–40 MHz).
- The strongest bursts have flux densities of 100–1000 Jy at the Earth. Individual bursts may exhibit variations of flux density up to four orders of magnitude below that value.

* Corresponding author.
E-mail address: akonov@ri.kharkov.ua (A.A. Konovalenko).

0019-1035/$ - see front matter © 2012 Elsevier Inc. All rights reserved.
http://dx.doi.org/10.1016/j.icarus.2012.07.024

- Duration of individual bursts stays between 30 ms and 400 ms.
- SED bursts are organized in episodes recurring with a periodicity about 10.6 h (close to Saturn's rotation period). Taking into account a combination of factors including storm visibility, radio emission beaming, Saturn's ionospheric cutoff, and detection threshold (in intensity), the duration of an SED episode is estimated to be between 1 and 5 h.
- The number of bursts in each episode varies from a few to hundreds.
- The overall long-term lightning activity at Saturn is sporadic and irregular. Activity occurs within intervals of a few weeks separated by several months of total inactivity. Since 2004 up to 2006 Cassini recorded six intervals of activity, named storms 0, A, B, C, D, E.
- Neither polarization nor frequency drift for the effective resolution (intrinsic or due to propagation) was detected yet for SED emission..

1.2. Previous attempts to detect SED from the ground

In spite of the fact, that SED flux densities can reach several hundreds of Jy at Earth (Fischer et al., 2006a; Zarka et al., 2006), previous attempts to detect them with ground-based radio telescopes (as listed below) have provided negative or ambiguous results so far. Before 2006, several attempts were made to detect SED from the ground. In particular,

(1) early observations of SED were made by Barrow in 1967 with the Arecibo dish (personal communication) at 16–18 MHz, using a narrow bandwidth (effective area $A_e \approx 10,000\ m^2$);
(2) SED observations were carried out by Abranin and Bazelyan in 1972 (personal communication) at 10–25 MHz using a filter bank at the UTR-2 radio telescope ($A_e \approx 100,000\ m^2$, observation bandwidth $\Delta f \approx 300$ kHz, integration time $\Delta t \approx 100$ ms);
(3) Carr et al. attempted to observe SED (observatory report, 1982) at 45 MHz with the Maipu array ($A_e \approx 6000\ m^2$, $\Delta f \approx 3$ MHz, $\Delta t \approx 30$ ms, i.e. 1σ sensitivity ≈ 30 Jy), and at 26.3 MHz with the Florida array ($A_e \approx 8000\ m^2$, $\Delta f \approx 500$ kHz, $\Delta t \approx 30$ ms, i.e. $1\sigma \approx 280$ Jy);
(4) a tentative detection was done during the Voyager 2 Saturn flyby by Lecacheux and Biraud (1984) at a wavelength of 21 cm using the Nancay decimeter radiotelescope;
(5) several observations campaign were carried out by Zarka et al. (1997) between 18 and 32 MHz at UTR-2, using a swept-frequency analyzer and an acousto-optical spectrograph (1σ sensitivity ≈ 10 Jy);
(6) observations in 2005 were performed at 20–25 MHz with UTR-2 by Sidorchuk et al. (2006), using an upgraded filterbank ($\Delta f \approx 3.5$ MHz, $\Delta t \approx 50$ ms, i.e. again 1σ sensitivity ≈ 10 Jy);
(7) simultaneously, an attempt was made by Zarka et al. (2006) at 21 MHz with the Nancay decameter array, using a digital receiver ($\Delta f \approx 10$ MHz, $\Delta t \approx 20$ ms, i.e. $1\sigma \approx 80$ Jy).

All these attempts had no success. Possible reasons are (i) sporadic/irregular character of SED; (ii) SED episodes with duration 1–5 h are recurrent every 10.66 h, and thus separated by several hours of apparent inactivity; (iii) burst rates within episodes are very variable, with some episodes consisting of only a few weak bursts. Taking into account the limited time durations of the above mentioned previous observations (several minutes to a few hours per day, a few days per month), absence of an a priori knowledge of ongoing lightning activity on Saturn, the limited sensitivity (Carr et al., 1982, $1\sigma \approx 280$ Jy) and very high observing frequency Lecacheux and Biraud (1984) of some of them, there was a low probability to detect strong enough SED radio bursts. Besides of that, SED radio search has to deal (as pointed out below in this paper) with a proper accounting of ionospheric propagation effects and interference (man-made and natural).

1.3. Interest of radio observations of planetary lightning

The basic interest to the planetary lightning studies is due to the information on atmosphere composition, geographical and seasonal variations, atmospheric physical processes (electrification, dynamics, production of organic molecules (Miller, 1953) (see e.g. Rinnert (1985) and Zarka et al. (2004) and references therein) they may give.

Investigation of low frequency radio emission associated with SED from the ground may enable the following:

(a) instantaneous broadband observations which are suitable for high "time-resolution" analysis of SED time profile and radio spectrum, even by using the wave-form registration;
(b) accurate localization of SED source and its association with Saturn by using long baseline interferometric measurements (angular resolution at 30 MHz with 1000 km baseline is 1″) gives us the additional criterion of the identification;
(c) stereoscopic ground-based + spacecraft observations may enable better determination of source position and directivity, and possibly view into Saturn's ionospheric propagation effects;
(d) furthermore, SED monitoring from Earth enable us to study Saturn's storm activity during the full planetary rotation.

Finally, the methodology developed for SED observations, which contains a technique for reliable detection of weak cosmic signals in presence of man-made radio frequency interference (RFI) and ionospheric effects, is applicable also to studies of active stars, pulsars, radio emission associated with X or γ bursts, and search for exoplanets at low frequencies. It is relevant for the existing and future (LOFAR, LWA, LSS, GURT, etc.) low-frequency instruments.

This paper describes the first, historical episode of SED successfully recorded from the ground; subsequent UTR-2 detections confirm the phenomena is ubiquitous (Zakharenko et al., 2011). These earliest observations were made with the UTR-2 radiotelescope, based on information about Saturn's lightning activity provided by Cassini/RPWS. The observations reported here began when the new storm 'E', which lasted from January 23 to February 24, 2006, detected by Cassini spacecraft. Instrument and method are described in Section 2. Results of the observations, which were carried out from January 29 to February 3 are reported in Section 3. Section 4 is devoted to the analysis of SED characteristics and their comparison with Cassini observations. Finally, the perspective for planetary lightning observations and new ground-based observations up to 2010 are briefly discussed.

2. Methods and equipment of the observations

Modern technical facilities, which are presently used in low frequency radio astronomy, enable detection of the radio emission from electrostatic discharges in Saturn's atmosphere. The central problem in such observations is a reliability.

Decameter frequency range is known for its high levels of the Galactic noise and interference. The knowledge of SED activity and the availability of SED pathfinder data from Cassini spacecraft are of particular importance.

2.1. Radio telescope and back-end facilities

The observations were carried out with the largest existing decameter radio telescope UTR-2 (Braude et al., 1978; Konovalenko, 2000). Many programmes have been carried out with this telescope, including the study of the quick-variable radio emission of Sun, Jupiter, pulsars, interplanetary scintillations, etc.

The distinctive properties of the UTR-2 radio telescope, which are important for the search for the radio emission from Saturn's lightning, are the following: the large linear size (2 km × 1 km), the large effective area ($A_{e(max)} = 150,000$ m^2 in the zenith direction), the high directivity ($\Theta \approx 30'$ at 25 MHz), the low level of the side lobes (< -13 dB) and the high radio frequency interference immunity (high dynamic range of the preamplifiers). There is also a possibility for electronic beam steering in a wide cone at all range of azimuth, as well as simultaneous observations with 5–8 spatially separated beams. The latter is important for setting ON–OFF modes. These modes are very effective for antennas like UTR-2. The mean level of the side lobes owing to the large number of the antenna elements (2040 dipoles) is small enough, i.e. $\delta_{s.l.} \approx 1/2040 \approx 5 \times 10^{-4}$. The high directivity also provides the small value of the ratio between solid angles of the main beam and the hemisphere $\Omega_A/2\pi \approx 10^{-6}$. From this it follows that the side lobe parameters (mainly in these directions radio frequency interferences are received) in ON and OFF modes show little difference, so radio frequency interference can easily be distinguished and even eliminated by subtraction during data processing. The radio telescope operates also with an effective control and calibration systems. Recently, the UTR-2 radio telescope has been sufficiently modernized and equipped with the most up-to-date receiver/analysis devices (Abranin et al., 2001).

The working scheme is illustrated in the block-diagram of the receiving system (Fig. 1). We used analog–digital filter-bank analyzers (Sidorchuk et al., 2006; Mel'nik et al., 2004). They operate in the radiometric mode and/or in the multiplicative mode using the correlation functionality of the UTR-2 radio telescope which consists of two orthogonal antennae: the North–South arm (dimensions of 1800 m × 60 m, 1440 elements) and the West–East arm (dimensions of 900 m × 60 m, 600 elements).

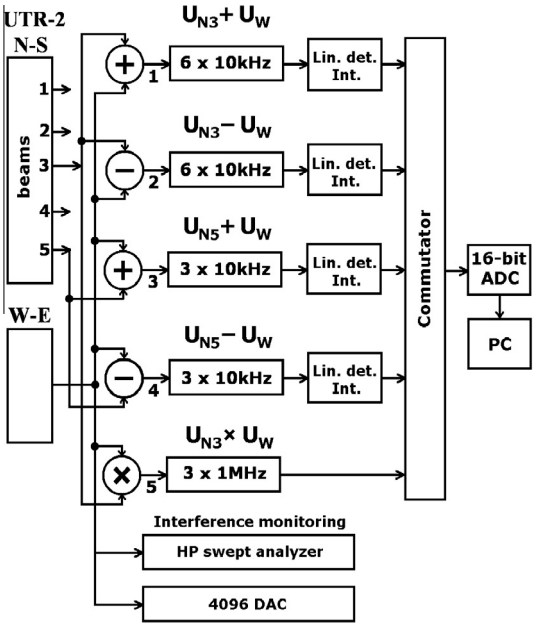

Fig. 1. A block diagram of the receiving configuration.

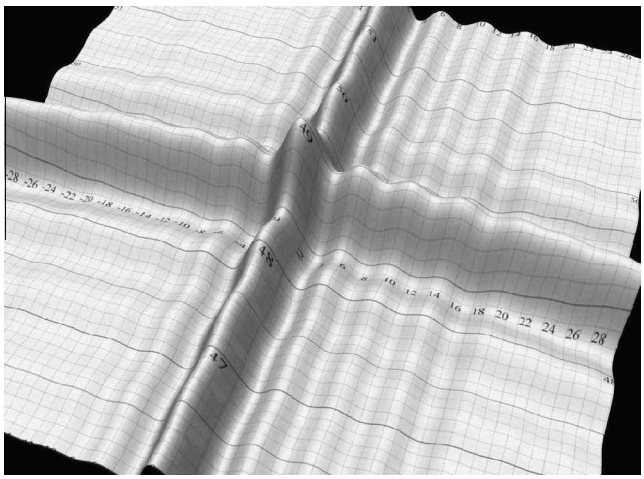

Fig. 2. The sum antenna pattern of the North–South and West–East arms.

Let us mark the waveform signals at the outputs of the North–South and West–East arms of UTR-2 as U_N and U_W, respectively. Then the instantaneous output of the radio telescope may be presented as follows:

1. ON_1 regime: $P_1 = (U_{N3} + U_W)^2$. The central beam of the North–South arm (N3) and the beam of the West–East arm are directed on the source (i.e. Saturn). The corresponding power antenna pattern (with the peak towards Saturn) is qualitatively presented in Fig. 2.
   The summed signal $(U_{N3} + U_W)$ is split into six radio receivers. The bandwidth of each is 10 kHz. The central frequencies of receivers 19.85; 20.14; 23.45; 23.75; 25.25; 25.75 MHz are chosen to minimize the interference level. Linear detectors and integrators are used at the output of each receiver. The signals are going through the commutator to the 16-bit ADC, and to the computer interface to be registered and stored on hard disk after squaring with sampling frequency of 50 Hz (the time resolution Δt is 20 ms).
2. OFF_1 regime: $P_2 = (U_{N3} - U_W)^2$. This is a case when the antenna pattern has zero level towards Saturn (see Fig. 3). Reception, amplification, transformation, registration and storage of the signal P_2 are similar to those as for signal P_1. Six separate receivers have the same frequencies.

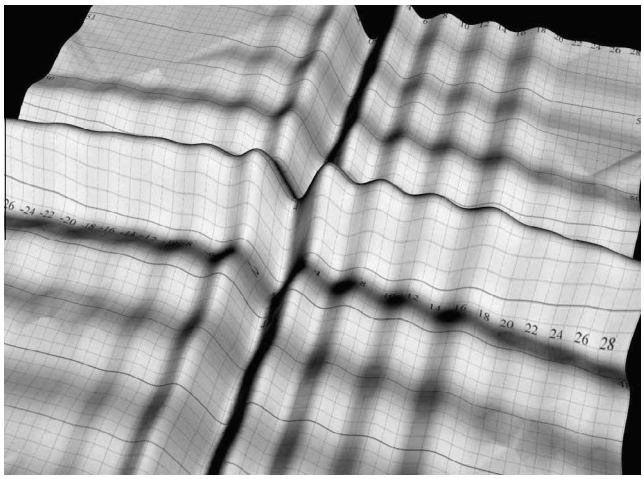

Fig. 3. The difference antenna pattern of the North–South and West–East arms.

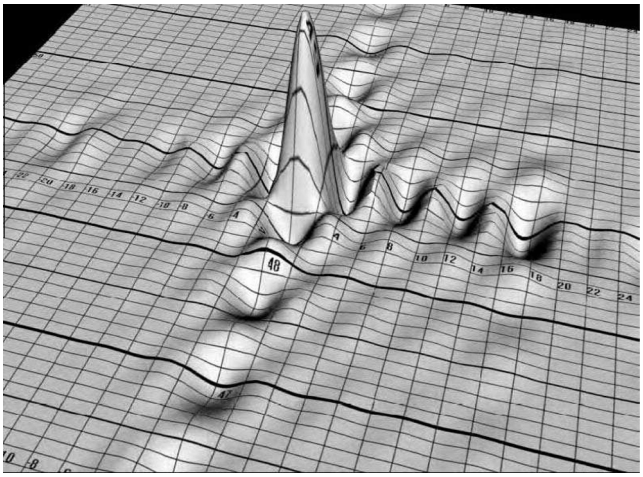

Fig. 4. The multiplied antenna pattern of the North–South and West–East arms.

3. ON_2 regime: the next value is calculated in a computer during real time registration:

$$P_3 = (U_{N3} + U_W)^2 - (U_{N3} - U_W)^2 \propto U_{N3}U_W = P_1 - P_2,$$

corresponding to a pencil beam of the power antenna pattern pointing at Saturn and presented in Fig. 4.

4. OFF_2 regime: a complimentary OFF regime is also formed to increase the reliability. The output signal is produced in a similar way as for P_3 but the beam $N5$ of the North–South arm is used. This beam is shifted by 1° relative to the central beam $N3$. Thus,

$$P_4 = (U_{N5} + U_W)^2 - (U_{N5} - U_W)^2 \propto U_{N5}U_W$$

The signal $(U_{N5} + U_W)$ is directed to three separate radio receivers with frequencies of 19.85; 23.45 and 25.25 MHz. The output signal $(U_{N5} - U_W)$ is connected to three other receivers with the same frequencies as used for $(U_{N5} + U_W)$. The procedures of registration and processing are similar to those as shown in items 1–3.

5. Regime ON_3: the additional increase of reliability and sensitivity is provided by using an independent (multiplicative) three-channel broad-band radiometer. In this case we have another ON regime with the pencil beam shown in Fig. 4 and described by $P_5 \propto U_{N3}U_W$.

The bandwidth of each channel in regime ON_3 is about 1 MHz, the central frequencies are 20.03; 23.57; 25.42 MHz and the time resolution and the sampling frequency are identical as given above. The block diagram shown in Fig. 1 also includes a swept analyzer and a digital correlometer for monochromatic interference signals monitoring.

The frequency range 20–25 MHz was chosen for observations of SED. This range does not have an overlap with the Cassini/RPWS frequency range (1–16 MHz), but it offers us at least two advantages. First, the maximum effective area of the UTR-2 radio telescope is realized below 25 MHz (above this edge A_e decreases significantly). Second, this range corresponds to not very high Galactic background temperatures, besides of that a low interference level and a rather weak ionospheric effect are typical for it. As the SED burst spectrum is nearly flat in the range 0.1–40 MHz, the chosen range is suitable for the SED radio emission detection on Earth.

The minimum detectable by a radio telescope flux density (σ-level) is well known to be determined by the relation:

$$\Delta S_{min} = \frac{2kT_{sys}}{A_e\sqrt{\Delta f \Delta t}}, \quad (1)$$

where k is the Boltzmann constant, T_{sys} is the system noise temperature (for the UTR-2 it is equal to the galactic background temperature), A_e is the effective area, Δf, Δt are the bandwidth and the time resolution, respectively.

During our experiments Saturn was close to the point with the equatorial coordinates $\alpha = 8^h40^m34^s$; $\delta = 19°2'$. For this direction the mean brightness temperature set by the background is about 20,000 K in the frequency range 20–25 MHz, the total effective area is about 100,000 m^2 and the time resolution is equal to 20 ms in all cases. So, for the narrow-band (NB) channel, $\Delta f = 10$ kHz, we have:

$$\Delta S_{min}(NB) \approx 40 \text{ Jy}, \quad (2)$$

and for the broadband (BB) one, $\Delta f = 1$ MHz, it is equal to:

$$\Delta S_{min}(BB) \approx 4 \text{ Jy}, \quad (3)$$

These values are reduced by the factor 2.4 and 1.7 by averaging over 6 and 3 channels correspondingly.

It is seen that the potential sensitivities of the narrowband and broad-band channels and the UTR-2 radio telescope parameters allow us to detect SEDs with the flux density of $\geqslant 50$ Jy with a rather high signal-to-noise ratio, especially in the broadband channel.

2.2. Sources and nature of pulsed interfering signals in the decametric range

Below we list the major types of interference which one has to deal with during the observations.

2.2.1. Man-made radio frequency interference (RFI)

Spontaneous electrical discharges (sparks) with the durations of 1 ms to 1 s are known to appear sporadically in the cable and control systems of antenna arrays. Discharges also appear at the instants when beam pointing is changed. However, as the occurrence of these interfering signals is known, they can be easily distinguished and eliminated from experimental data. Other interference may arise from general and special equipment when it is switched on and off. The duration of the corresponding pulses is about 100 ms.

Another type of the human generated noise is the external interference. Pulsed decametric radio emission comes from broadcast services, radar and remote sensing systems, car ignitions etc. The appropriate location of the UTR-2 radio telescope in a radio quiet zone, far enough from the large town (70 km) and villages, minimizes their effect on the radio telescope systems. Monochromatic radio emission arising from HF broadcast stations is not so difficult to exclude, but the antenna system and back-ends must have high dynamic ranges to allow an appropriate detection of both weak astronomical and very strong interfering signals. In addition to this, a considerable care must be taken to avoid intermodulation distortion.

2.2.2. Naturally occurring interference

Examples of naturally occurring interference include:

- terrestrial lightning (the durations of ≈1 ms, the flux density sharply decreases with frequency, there is no frequency drift);
- radio emission arising from atmospheric showers of high energy cosmic rays (the duration is less than 1 μs);
- terrestrial lightning-like transient phenomena (durations vary within the wide range) e.g. "sprites" (Franz et al., 1990; Sentman et al., 1995; Rodger et al., 1998), transionospheric pulse pairs (Holden et al., 1995) and subionospheric pulse pairs (Smith and Holden, 1996);

- variable pulsed radio emission coming from cosmic radio sources (Sun, Jupiter, pulsars), interplanetary scintillations of compact radio sources. The signals arising from these sources and SED bursts differ in a range of parameters, including: duration, spectrum, frequency drift. Therefore, they can be easily separated by existing appropriate methods.

Given that there exist many sources of the radio frequency interference in the decametric range, for the detection of SED bursts, one have necessary to use appropriate antenna systems, back-end devices and methods.

2.3. SED detectability criteria

The methods of observations proposed above and logical speculations enable us to formulate the following criteria for reliable detection of SED signals with expected parameters (as described in Section 1.1) in the presence of interference:

1. Presence of the signal in ON_1 regime.
2. Absence in OFF_1 regime.
3. Presence in ON_2 regime.
4. Absence in OFF_2 regime.
5. Presence in the independent receiving device, ON_3 regime.
6. Presence in all frequency channels of all receivers in the range 20–25 MHz of ON_1, ON_2 and ON_3 regimes.
7. Absence of evident frequency drift.
8. Positive polarity of the events (interference signals can be negative in ON_2 and ON_3 regimes).
9. Moderate intensity (< 1000 Jy).
10. Moderate duration (> 20 ms, < 1 s).
11. Rather strong surpass of the noise fluctuation level ($> 5\sigma$).
12. Absence at far distances from Saturn's position in the sky (with the same antenna beam position relatively to the Earth).
13. Absence in the calibration regime when a noise generator is connected to the input of the receiving system instead of the antenna.
14. Presence of more than one event during rather long observations (>10 h).
15. Simultaneous presence at distant antennas, for example, URAN or Nancay array (this criterion does not apply in our investigation).
16. Coincidence with Cassini observations, taking into account the radio propagation delay and Saturn–Cassini–Earth position (in particular, SED bursts are organized in episodes with the duration <5 h and the periodicity of about 10.66 h).

We considered each of criteria 1–16 as a necessary but not sufficient condition. Criteria 1–14 and 16 were checked simultaneously for making a conclusion about the detection. All criteria had to be satisfied for SED detection to be confirmed. Criterion 15 did not use. Such approach provides practically 100% reliability of the SED detection fact. I.e., the probability of any artifact detection is close to zero. It should be noted, that there is some probability of loss of observation due to the effect of the ionosphere and the interplanetary plasma on signal propagation. The ionospheric refraction can shift Saturn away from the antenna beam axis, and criteria 1, 3, 5, 12 will be broken. Also, the SED bursts registered onboard Cassini may appear to be sufficiently reduced in intensity at Earth due to the interplanetary scintillations with high index. These effects make it difficult to compare the events, detected onboard Cassini, and those observed at Earth (criterion 6). However, the authors' broad experience in low-frequency radio astronomy suggests that the mentioned above effects can distort not more than 20% of the useful information at the frequencies from 20 to 30 MHz.

The criteria introduced above (i.e., a multi-comparing ON–OFF approach) were successfully tested with the UTR-2 radio telescope during the search and investigation of weak astrophysical signals (e.g., recombination lines, flare stars, pulsar radio emission, etc.).

3. Observations and results

3.1. Description of the experiment

The reported search of the SED radio emission was started at the end of January 2006 immediately after the information from Cassini/RPWS instrument about the beginning of the ordinary storm (E-storm) at Saturn was received (Konovalenko et al., 2006). Due to winter ionospheric conditions, low level of interference, absence of local lightning activity, this time was rather favorable for observations at decameter wavelengths, for the SED search particularly. The time of Saturn's culmination was near the local midnight which additionally minimized the negative effects. Also, Earth was at the minimum distance to Saturn ($d \approx 9$ AU). Furthermore, during this epoch Saturn's position in the sky ($\alpha = 8^h40^m34^s$; $\delta = 19°2'$) belonged to the region with the lowest temperature of the galactic background $T_{bg}(20\text{—}25\ \text{MHz}) \approx 20,000$ K which improved the experimental sensitivity. Altogether, the brightness temperature of the galactic background is known to change several times while Saturn moves around Sun. These changes of the brightness temperature have similar effect as the reduction of the effective antenna area. The geometry of the experiment is presented in Fig. 5.

The observations were carried out with the UTR-2, using the methods, described above. They consisted of five sessions in the period from January 29 to February 3, 2006. The duration of each session was about ± 3 h from culmination time. During these sessions the planet was steered electronically by the UTR-2 beam with a step of 2 min. This corresponds to $\approx 10'$ in the sky. Diurnal data are registered continuously in a computer. An ethalon noise generator with the variable output of the signal level was connected onto the equipment before each session to estimate the flux density and to realize criterion 13. Occasionally, the radio source 3C144 with close declination and rather far right ascension was observed to obtain the intensity independently and to realize criterion 12. Total duration of all sessions was about 40 h.

3.2. Examples of SED detection

The obtained data were analyzed with different computer algorithms and also visually, according to the proposed criteria. Firstly,

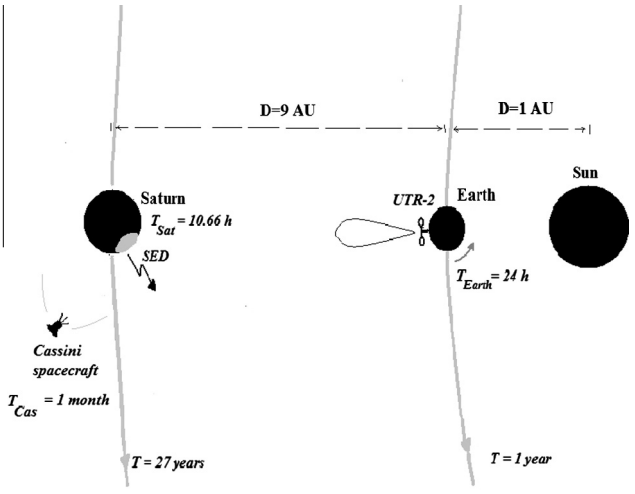

Fig. 5. The geometry of the experiment.

the events with an intensity of more than 5σ were extracted from the broadband channel data (ON_3 regime). Secondly, the extracted events were compared with the narrowband channel data in the regimes ON_1; ON_2 and OFF_1; OFF_2 taking into account the lower sensitivity of these channels. Finally we analyzed whether the events are consistent with all other criteria. Eventually 69 events from all data were selected as SED bursts in accordance with all criteria and about 30 bursts were attributed to interference pulse signals.

The example of a signal record with SED features is presented in Fig. 6 (axis of ordinates are shown in arbitrary units) for all regimes ON_1, OFF_1, ON_2, OFF_2, ON_3 and for all frequency channels. Bottom line on all panels is a result of averaging all the top ones. It is seen, that the records contain two pulses which correspond to the SED signals with rather high signal-to-noise ratio (they are near 22:01:48 and 22:01:56 UT 30 January 2006). All criteria are fulfilled including the main ones (criteria number 1–14). The examples of other three individual SED signals in the narrowband (ON and OFF regimes, same date) and broadband channels are presented in Fig. 7a–c.

3.3. Main SED parameters

The intensity distribution of SED signals detected during our observations is presented in Fig. 8. The cut-off of the dependence

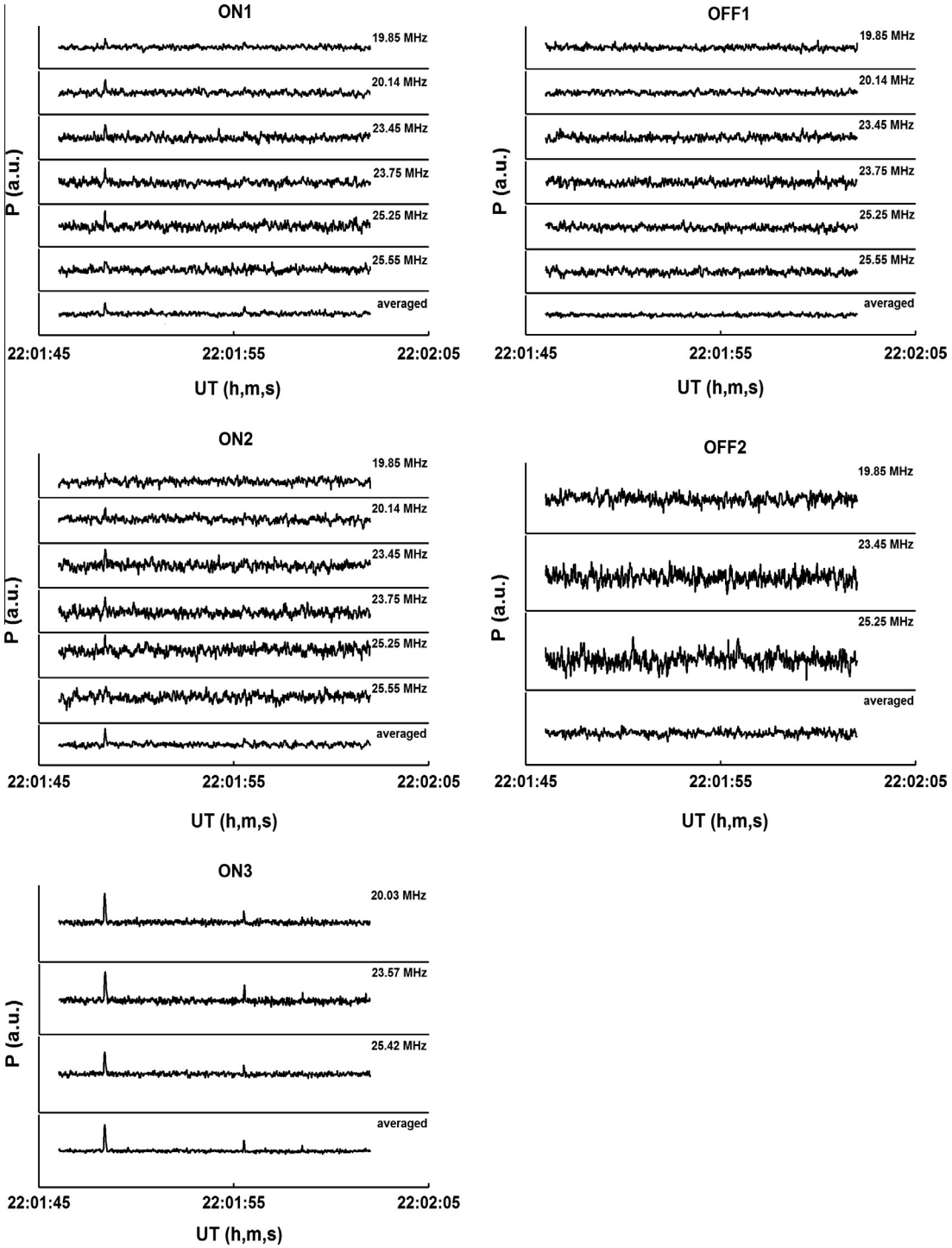

Fig. 6. The example of a signal record (30 January 2006) with SED features.

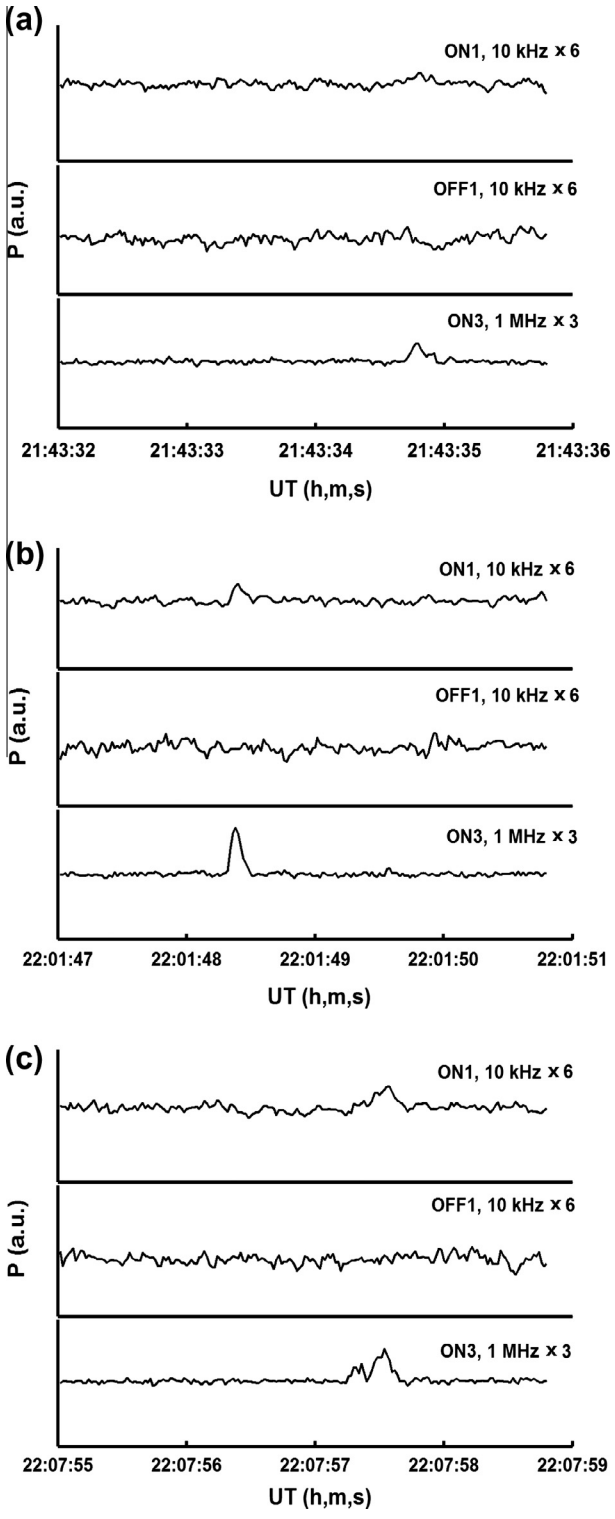

Fig. 7. The examples (30 January 2006) of individual SED signals in the narrowband (ON and OFF regimes) and broadband channels.

($S < 50$ Jy) is determined by the evident detection threshold. The intensity of some detected bursts on the Earth's surface reached about 700 Jy.

The distribution of burst durations (full width at half maximum) was determined with time step of 20 ms is shown in Fig. 9. It can be described by an exponential law with e-folding

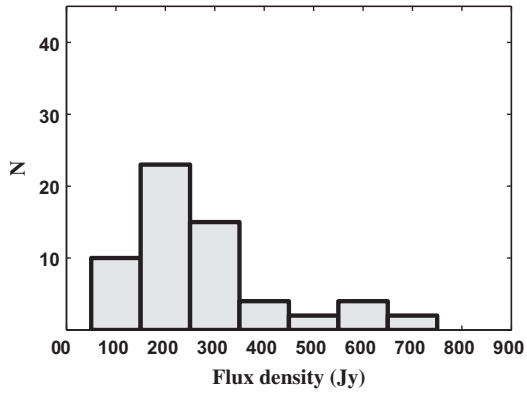

Fig. 8. The intensity distribution of the detected SED bursts.

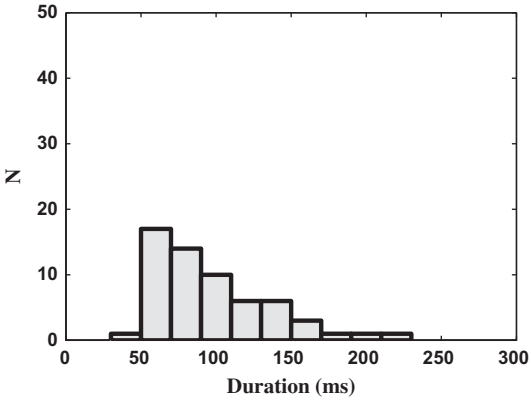

Fig. 9. The duration distribution of the detected SED bursts.

time 45 ± 5 ms. As one can see burst durations vary from 60 ms to 220 ms.

Therefore, we were able, using ground-based observations, to reliably detect a rather big set of the SED signals. The consideration of one of the most important criteria (coincidence with Cassini data, criterion 16), as well as investigation of some other properties of the SED burst detected with the ground-based instrument are provided in the next section.

4. Discussion

4.1. Comparison with Cassini data

The analysis of the experiment's geometry (see Fig. 5), taking into account position of Cassini and Saturn's rotation period (T_{Sat}), enable performing the following estimations. The observations of the same SED events (during a full episode) at UTR-2 and Cassini are possible only if the spacecraft is situated at line of sight Saturn–Earth. In common case (as it was in these experiments) a difference between an episode arising at Cassini and Earth is equal to the time of Saturn rotation (T_{rot}) by an angle Cassini–Saturn–Earth ($\alpha_{C-S-E} \approx 117^\circ$) derived from Cassini position (Fischer et al., 2007) using the expression $T_{rot} = (\alpha_{C-S-E}/360^\circ)T_{Sat} \approx 3.46$ h. (In the following we neglect Cassini's movement along its orbit during 5 days.) Simultaneous observations onboard Cassini and on the Earth's surface are possible during $T_{sim} = T_{Sat}/2 - T_{rot} \approx 1.87$ h. In the records of the UTR-2 the start of an episode is additionally shifted by the signal propagation time $T_{Cas-Earth} \approx 1.12$ h

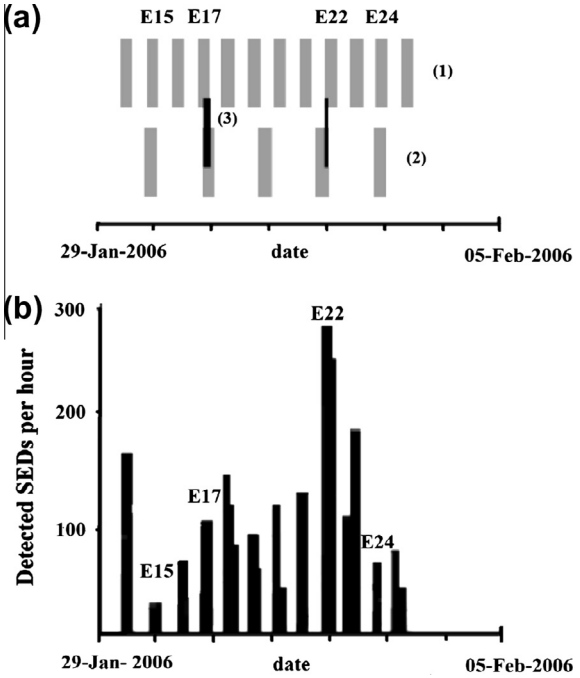

Fig. 10. The episodes of storm E registered by means of Cassini/RPWS and the sessions of observations at UTR-2; (a) (1) interpolated times of episodes E14–E25 registered onboard Cassini taking into account time delay $T_{Cas-Earth}$, (2) the sessions of observations carried out at UTR-2, (3) two time intervals of simultaneous observations; (b) number of SEDs per hour for each episode registered onboard Cassini.

and at the end of January 2006 the total delay is $T_{rot} + T_{Cas-Earth} \approx 4.6$ h.

Fig. 10a shows: (1) interpolated Earth receiving times for episodes E14-E25 registered onboard Cassini taking into account the total time delay; (2) the time intervals of the UTR-2 observations and (3) the time intervals (two) where the SED bursts have been registered with the UTR-2 radio telescope. There is a good agreement between the space and Earth-based detections for episodes E17 and E22. The absence of the Earth-based SED detections in other favorable time intervals (episodes E15 and E24) can be explained probably by lower SED activity (see Fig. 10b). The absence of the Earth-based SED detections during episodes E19 and E20 can be easily explained by the stop of the UTR-2 operation.

The comparison of an individual SED burst detected on the Earth's surface and onboard Cassini is a more difficult task, which requires a precise time synchronization and precise trajectory parameters. This, however, was out of scope of the planned experiments. Nevertheless, at least two SED bursts, detected on the ground at 23 h 34 m 26.880 s UT and 23 h 42 m 15.420 s UT 30 January 2006, coincide with the SED bursts detected onboard Cassini for the short time period of episode E22 (about 1.5 h) when the observations of the same SED signals in parallel with Cassini/RPWS as well as with the UTR-2 were in principle possible.

Thus, this comparative analysis of ground-based and space-borne data finally confirms the fact that SED detection is possible by using Earth-based facilities.

4.2. Intensity and duration of SEDs

As pointed out in Fig. 8, the intensities of the SED bursts detected on the Earth's surface vary over the range from 50 to 700 Jy. This range agrees well with the previous estimations 0.4–1000 Jy (Zarka et al., 2004, 2006). The burst intensity was determined by using standard methods for data calibration for the UTR-2 radio telescope, which are based on the use of a precise noise generator and/or the observations of the radio source 3C144 with the known flux density $S_{3C144}(25\ \text{MHz}) = 3000$ Jy. The accuracy of the flux density estimation is about 20%.

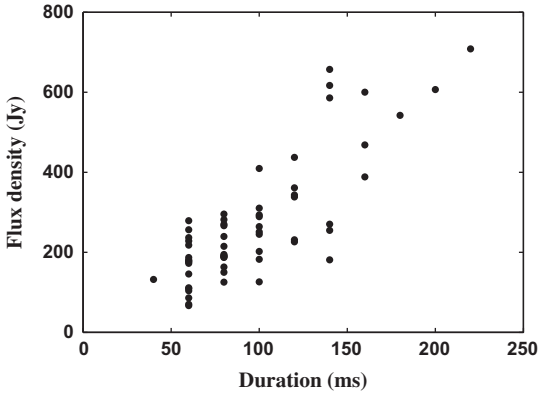

Fig. 11. Flux density vs duration for the detected SED bursts.

As the whole time interval of SED bursts observation is about 60 min (see Fig. 10), the number of events with $S > 50$ Jy per minute is $N(S > 50\ \text{Jy}) \approx 69/60 \approx 1.2\ \text{min}^{-1}$, where 69 is the total number of the observed bursts.

It is easy to calculate the source maximum spectral power on Saturn by using the maximum flux density (700 Jy) observed on the ground:

$$P_{max} = 4\pi d_{Earth}^2 S_{max} \approx 500\ \text{W/Hz}, \quad (4)$$

where d_{Earth} stays for Earth–Saturn distance.

This result is in agreement with that, obtained for storms 0-D by Fischer et al. (2006a) and Zarka et al. (2006) (the average SED source spectral power is about 50–100 W/Hz and the strongest bursts may exceed five times this value).

As it was mentioned above, our results show that the durations of the detected bursts lie from 60 ms to 220 ms. This agrees with the time range of Cassini data for storm E (35–490 ms) (Fischer et al., 2007). The distribution of burst durations exhibits an exponential decrease with an e-folding time of 45 ± 5 ms, when Cassini result is 49 ± 3 ms (Fischer et al., 2007).

Fig. 11 shows the intensity versus the duration for all detected bursts. The dependence is also analogous to that obtained for the space-borne data.

It should be emphasized that during January 29–February 3 (DOY29–DOY34, episodes E15–E24) about 1000 SED bursts were detected by Cassini/RPWS. This is much more than the number of the SED bursts detected on the ground. The reasons are evident. The maximum flux density at Cassini's position is:

$$S_{max} = \frac{P_{max}}{4\pi d_{Cas}^2} \approx 10^8\ \text{Jy}, \quad (5)$$

The last value is five orders of magnitude higher than at Earth due to much smaller distance ($d_{Cas} \approx 0.02$ AU; $d_{Earth} \approx 9$ AU). In spite of the huge effective area of the UTR-2 ($A_{eUTR-2}/A_{eCas} \approx 10^3$), the antenna temperature from the bursts ($T_A = SA_e/2k$) at the output of the UTR-2 is one hundred times lower than at the output of Cassini's antenna. So, if a burst level exceeds the background level on Cassini by 10–20 dB, for UTR-2 it will be lower than the background level by 10–0 dB. Furthermore, the Cassini spacecraft observed SED episodes every 10.66 h while the UTR-2 radio telescope managed to do this only when Saturn is over the Earth's horizon. Thus, during the analysis of the SED bursts properties we actually compared the Earth-based and space-borne data only for intense events observed onboard Cassini.

4.3. Absorption, dispersion and broadening of the SED radio emission

In the previous discussion we took into account mainly such differences in the ground-based and space-borne experiments as different distances and the geometry of the observations. At the same time, additional well-known effects arise when radio waves propagate through a plasma. These effects increase at low frequencies, especially at decameter wavelengths and include in particular absorption, dispersion and broadening of pulse signals. Here we would like to establish whether or not the medium (the interplanetary plasma and the terrestrial ionosphere) between Saturn and the ground-based radio telescope essentially influences SED signals parameters.

If the brightness temperature of the source radio emission before entry the plasma layer is T_s , after passing the plasma layer we have:

$$T_{obs} = T_s e^{-\tau}$$

where τ is the optical depth of the plasma layer. It is equivalent to:

$$\tau = \int_0^L 3.14 \times 10^{-2} \frac{N_e^2 L}{T_e^{3/2} f^2} [1.5 \ln T_e - \ln(20.18 f)] dl, \quad (6)$$

where L is the depth of the plasma layer in pc, f is the frequency of observations in GHz, l is the coordinate along the line of sight, N_e and T_e are the electron density and the electron temperature, respectively. In common case N_e and T_e are functions of the coordinate l. For the typical parameters of the interplanetary medium and the ionosphere and for the distance between Saturn and the Earth of about 9 AU we have $\tau < 10^{-3}$. So it is negligible and does not have any effect on signal amplitude.

The time delay which depends on frequency can be written for two frequencies as (Zarka et al., 1997)

$$t(f_1) - t(f_2) = 4.15 \times 10^6 \, \mathrm{DM} (f_1^{-2} - f_2^{-2}) \quad (7)$$

with t in ms, f in MHz and DM being the dispersion measure in pc cm^{-3}. In our case even for particle density 1 cm^{-3} DM $\approx$ 9 AU cm^{-3} $\approx 5 \times 10^{-5}$ pc cm^{-3}, thus, the resulting dispersion is negligible ($\approx$1.5 ms) even between $f_1 \approx 10$ MHz (Cassini) and $f_2 \approx 20$ MHz (UTR-2). It is sufficiently less than the observed pulses width (50–250 ms) and temporal resolution (20 ms). The corresponding temporal broadening is also very weak, less than a ms at $f < 30$ MHz.

The coincidence of SED pulses at frequencies 20 MHz and 25 MHz, as was observed by the UTR-2, shows the absence of clear frequency drift during the SED signal generation. It is not so evident from space data, because they are obtained with a swept spectrum analyzer in contrary to the parallel analyzers at the UTR-2.

As it follows from the above analysis, the medium propagation effects at 10–30 MHz can influence ground-based observations of SED only as refractive and scintillation phenomena. The time delay and broadening (with the time resolution reached in 2006), as well as absorption effects are negligible. That enables the high accuracy of ground-based observations and their comparison with space-born experiments.

5. Conclusions and perspectives

This paper describes the first successful recording of the radio signals from Saturn's lightning by using ground-based observations. Subsequent UTR-2 SED detections confirm the phenomena is ubiquitous (Zakharenko et al., 2011) and thereby open a new field of planetary radio emission accessible from the Earth. The historical first positive result was obtained, first of all, due to the information from the Cassini spacecraft about the beginning of a giant SED activity (E-storm) at the end of January 2006. When this information was received, the ground-based search at frequencies between 20 and 25 MHz was immediately started on the largest decameter wavelength radio telescope UTR-2. The storm lasted from 25 January to 2 February 2006. The implemented means and methods including careful selection criteria,based on the comparison of simultaneous ON/OFF observations allow to detect reliably 69 radio bursts (for two episodes at least). Their parameters, e.g., maximal flux densities are (up toseveral hundred Jy), burst durations (between 60 and 220 ms) are in good agreement with Cassini data, as well as with the previous estimations and predictions for the ground-based observations.

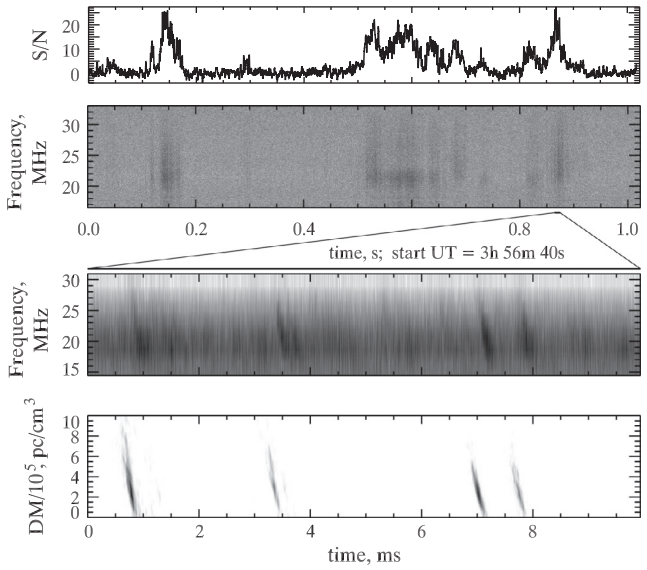

Fig. 12. Relative intensity S/N and dynamic spectra at frequencies 15–33 MHz. Dispersion time delay of the short pulses between 15 and 30 MHz at the level of few tens of microseconds. It corresponds to the dispersion measure of $\approx 2.6 \times 10^{-5}$ pc cm^{-3}. These data are from the UTR-2 SED detection as reported in Zakharenko et al. (2012).

It is important to emphasize that the methods and identification criteria, what were developed, implemented and described in this paper for E-storm, are used in the UTR-2 observations of the following SED storms. After 2006 up to 2011 Cassini detected the storms named F–J (Fischer et al., 2011a,b). New observations on the UTR-2 were carried out during this period with more effective 8192-channel digital spectral processors at the back-end, which enable realizing a waveform regime, when a time resolution is practically not limited (nanosecond level) (Ryabov et al., 2010; Konovalenko et al., 2011). The capabilities of this facility are much better than those of the previous ones (e.g., filter-bank, implemented during E-storm). In particular, it enable a broader instant continuous frequency band (0–33 MHz), better time and frequency resolution (1 ms and 4 kHz, respectively), more dynamic range and interference immunity. Also we significantly improve methods used for observations and data processing. As a result, now the achieved sensitivity is less then 1 Jy. That is much closer to Cassini capability (from the SED detectability point of view). Many new results were obtained during these investigations. Careful comparing of more than 1000 SEDs detected on Cassini and UTR-2 was conducted. Characteristics of SED radio emission such as spectra in the frequency band 12–33 MHz, fine time structure (at microsecond level), and dispersion delay were studied (Zakharenko et al., 2011, 2012; Grießmeier et al., 2011a,b).

Fig. 12, from the observations discussed by Zakharenko et al. (2012) illustrates the dynamic spectra at frequencies from 15 to 33 MHz (after the Fourier transform of the waveform record) for

the time interval of 1.2 s (top) and its zoom for 10 ms (bottom) near 3:56:40 UT 23 December 2010 during J-storm. For the first time we can see very reach fine time structure of the SED due to very high resolution. Furthermore we detected evident time delay of the short pulses between 15 and 30 MHz at the level of few tens of microseconds. Accordingly to (7), it corresponds to the dispersion measure of $\approx 2.6 \times 10^{-5}$ pc cm^{-3}. These new experiments give us an additional criterium for the identification of the SED signals on the ground (e.g., Earth lightning signals do not show dispersion), and open new possibilities for the SED studies with high performance facilities and methods. Many corresponding experimental data are still in at the stage of the processing and analysis.

Future planetary space missions, including planetary lightning investigations, will offer exploratory studies, while ground-based radio observations may complement them, by performing on instantaneous broad-band measurements with high temporal-frequency resolution for time profile and radio spectrum of the lightning signal. This possibility is proved now for Saturn (SED), and expected, that Uranus lightning (UED) can be observed from the ground too. It is important also to re-asses/confirm lightning activity at Venus and Titan, as well as to check the existence of Martian and Jupiter discharges, and possible transient activity at Neptune (Zarka et al., 2008; Grießmeier et al., 2011a). In case of successful detection, the physical properties of planetary radio discharges can be studied in detail.

Ground-based observations of planetary lightning radio signal are also of methodological interest for the search of weak sporadic (transient) astrophysical phenomena at low frequencies (decameter–meter wavelengths) in the presence of intense man-made and natural interferences and ionosphere effects. This methodology is applicable and should be of interest for existing and future low-frequency instruments like UTR-2, URAN (Ukraine), Low Frequency Array – LOFAR (the Netherlands), E-LOFAR (Europe), LOFAR Super Station – LSS (France), Giant Ukrainian Radio Telescope – GURT (Ukraine), and Long Wavelength Array – LWA (USA).

Acknowledgments

This work was initiated and partly supported by ANR Program NT05-1 42530 "Radio-Exopla", and pursued in the frame of the NASU-CNRS PICS Program "Development of LF radioastronomy with ultrahigh sensitivity and resolution" (Grant 1.33.11). This work is also partially supported by the Ukrainian State Fund for Fundamental Researches (Project F28.2/005). Cassini activities in LESIA are supported by the CNES (Centre National d'Etudes Spatiales). This work is also supported by the National Academy of Sciences of Ukraine and the Russian Foundation for Basic Research (Ukrainian–Russian Project 2012). We thank both the referees for the very useful comments.

References

Abranin, E.P., Bruck, Yu.M., Zakharenko, V.V., Konovalenko, A.A., 2001. The new preamplification system for the UTR-2 radio telescope. Exp. Astron. 11, 85–112.
Braude, S. Ya., Megn, A.V., Sodin, L.G., 1978. Decameter wavelength radio telescope UTR-2. Antennas 26, 3–15 (in Russian).
Evans, D.R., Warwick, J.W., Pearce, J.B., Carr, T.D., Schaube, J.J., 1981. Impulsive radio discharges near Saturn. Nature 292, 716–718.
Fischer, G., Desch, M.D., Zarka, P., Kaiser, M.L., Gurnett, D.A., Kurth, W.S., Macher, W., Rucker, H.O., Lecacheux, A., Farrell, W.M., Cecconi, B., 2006a. Saturn lightning recorded by Cassini/RPWS in 2004. Icarus 183, 135–152.
Fischer, G. et al., 2006b. On the intensity of Saturn lightning. In: Rucker, H.O., Kurth, W.S., Mann, G. (Eds.), Planetary Radio Emissions VI. Austrian Academy of Sciences Press, Vienna, pp. 123–132.
Fischer, G., Kurth, W.S., Dyudina, U.A., Kaiser, M.L., Zarka, P., Lecacheux, A., Ingersoll, A.P., Gurnett, D.A., 2007. Analysis of a giant lightning storm on Saturn. Icarus 190, 528–544.
Fischer, G. et al., 2011a. A giant thunderstorm on Saturn. Nature 475, 75–77.
Fischer, G. et al., 2011b. Overview of Saturn lightning observations. In: Rucker, H.O., Kurth, W.S., Louarn, P., Fischer, G. (Eds.), Planetary Radio Emissions VII. Austrian Academy of Sciences Press, Vienna, pp. 135–144.
Franz, R.C., Nemzek, R.J., Winckler, J.R., 1990. Television image of a large upward electrical discharge above a thunderstorm system. Science 249, 48.
Grießmeier, J.-M. et al., 2011a. Ground-based study of Saturn lightning. In: Rucker, H.O., Kurth, W.S., Louarn, P., Fischer, G. (Eds.), Planetary Radio Emissions VII. Austrian Academy of Sciences Press, Vienna, pp. 145–154.
Grießmeier, J.-M., Zarka, P., Girard, J.N., 2011b. Observation of planetary radio emissions using large arrays. Radio Sci. 46, RS0F09.
Holden, D.N., Munson, C.P., Devenport, J.C., 1995. Satellite observations of transionospheric pulse pairs. Geophys. Res. Lett. 22, 889–892.
Konovalenko, A.A., 2000. Ukraine decameter wave radio astronomy systems and their perspectives, radioastronomy at long wavelengths. Geophysical Monograph 119, American Geophysical Union, pp. 311–319.
Konovalenko, A.A. et al., 2006. Ground-based decameter wavelength observations of Saturn electrostatic discharges. European Planetary Science Congress 2006, EPSC2006-A-00229.
Konovalenko, A.A. et al., 2011. New antennas and methods for the low frequency stellar and planetary radio astronomy. In: Rucker, H.O., Kurth, W.S., Louarn, P., Fischer, G. (Eds.), Proceedings of Planetary Radio Emissions VII. Austrian Academy of Sciences Press, Vienna, pp. 521–531.
Lecacheux, A., Biraud, F., 1984. An Earth-based attempt to detect SED at 21 centimeters. In: Brahic, A. (Ed.), Planetary Rings. Cepadues/CNES, pp. 319–324.
Mel'nik, V.N. et al., 2004. Observations of solar type II bursts at frequencies 10–30 MHz. Solar Phys. 222 (1), 151–166.
Miller, S.L., 1953. A production of amino acids under possible primitive Earth conditions. Science 117, 528–534.
Rinnert, K., 1985. Lightning on other planets. J. Geophys. Res. 90, 6225–6237.
Rodger, C.J., Wait, J.R., Dowden, R.L., Thomson, N.R., 1998. Radiating conducting columns inside the Earth-ionosphere wave-guide: Application to red sprites. J. Atmos. Solar – Terr. Phys. 60, 1193–1204.
Ryabov, V.B. et al., 2010. A low-noise, high-dynamic-range, digital receiver for radio astronomy applications: An efficient solution for observing radio-bursts from Jupiter, the Sun, pulsars, and other astrophysical plasmas below 30 MHz. Astron. Astrophys. 510, A16.
Sentman, D.D., Wescott, E.M., Osborne, D.L., Hampton, D.L., Heavner, M.J., 1995. Preliminary results of the sprites 94 aircraft campaign: red sprites. Geophys. Res. Lett. 22, 1205–1208.
Sidorchuk, K.M. et al., 2006. Search of non-thermal radio emission from planets and stars at decameter wavelength. In: Rucker, H.O., Kurth, W.S., Mann, G. (Eds.), Planetary Radio Emissions VI. Austrian Academy of Sciences Press, Vienna, pp. 83–84.
Smith, D.A., Holden, D.N., 1996. Ground-based observations of subionospheric pulse pairs. Radio Sci. 3, 553–571.
Warwick, J.W. et al., 1981. Planetary radio astronomy observations from Voyager 1 near Saturn. Science 212, 239–243.
Zakharenko, V.V. et al., 2011. Identification of Saturn lightnings recorded by the UTR-2 radio telescope and Cassini spacecraft. Radio Phys. Radio Asrton. 2, 93–98.
Zakharenko, V. et al., 2012. Ground-based and spacecraft observations of lightning activity on Saturn. Planet. Space Sci. 61, 53–59.
Zarka, P., Pedersen, B.M., 1983. Statistical study of Saturn electrostatic discharges. J. Geophys. Res. 88 (A11), 9007–9018.
Zarka, P., Pedersen, B.M., 1986. Radio detection of uranian lightning by Voyager 2. Nature 323, 605–608.
Zarka, P. et al., 1997. Ground-based high sensitivity radio astronomy at decameter wavelengths. In: Rucker, H.O., Bauer, S.J., Lecacheux, A. (Eds.), Planetary Radio Emissions IV. Austrian Academy of Sciences Press, Vienna, pp. 101–127.
Zarka, P., Farrell, W.M., Kaiser, M.L., Blanc, E., Kurth, W.S., 2004. Study of Solar System planetary lightning with LOFAR. Planet. Space Sci. 52, 1435–1447.
Zarka, P. et al., 2006. Physical properties and detection of Saturn's radio lightning. In: Rucker, H.O., Kurth, W.S., Mann, G. (Eds.), Planetary Radio Emissions VI. Austrian Academy of Sciences Press, Vienna, pp. 111–122.
Zarka, P., Farrell, W., Fischer, G., Konovalenko, A., 2008. Ground-based and space-based radio observations of planetary lightning. Space Sci. Rev. 137, 257–269.